THE ASTROPHYSICAL JOURNAL, 564:8–14, 2002 January 1

PREDICTING THE NUMBER, SPATIAL DISTRIBUTION, AND MERGING HISTORY OF DARK MATTER HALOS

PIERLUIGI MONACO,[1] TOM THEUNS,[2] GIULIANO TAFFONI,[3] FABIO GOVERNATO,[4] TOM QUINN,[5] AND JOACHIM STADEL[5]

Received 2001 April 30; accepted 2001 September 4

ABSTRACT

We present a new algorithm (PINOCCHIO: pinpointing orbit-crossing collapsed hierarchical objects) to accurately predict the formation and evolution of individual dark matter halos in a given realization of an initial linear density field. Compared with the halo population formed in a large (360^3 particles) collisionless simulation of a cold dark matter (CDM) universe, our method is able to predict to better than 10% statistical quantities such as the mass function, two-point correlation function, and progenitor mass function of the halos. Masses of individual halos are estimated accurately as well, with errors typically of order 30% in the mass range well resolved by the numerical simulation. These results show that the hierarchical formation of dark matter halos can be accurately predicted using local approximations to the dynamics when the correlations in the initial density field are properly taken into account. The approach allows one to automatically generate a large ensemble of accurate merging histories of halos with complete knowledge of their spatial distribution. The construction of the full merger tree for a 256^3 realization requires a few hours of CPU time on a personal computer, orders of magnitude faster than the corresponding N-body simulation would take, and does not need any extensive postprocessing. The technique can be efficiently used, for instance, for generating the input for galaxy formation modeling.

Subject headings: cosmology: theory — dark matter — galaxies: clusters: general — galaxies: formation — galaxies: halos

1. INTRODUCTION

In currently favored, dark matter dominated cosmological models, initially small density fluctuations are amplified by gravity and eventually condense out of the Hubble expansion to form gravitationally-bound systems at a density contrast of $\gtrsim 200$ dark matter halos (e.g., Peebles 1993). The properties of the halo population are of fundamental importance for understanding galaxy formation and evolution. Indeed, galaxies are thought to form when baryons fall into such dark matter halos and are shocked to sufficiently high temperatures and densities that the gas can cool radiatively to form stars (Rees & Ostriker 1977; White & Rees 1978).

The formation of halos can be studied using numerical simulations which usually evolve a set of equal mass particles that represent the dark matter in a periodic simulation box (e.g., Efstathiou et al. 1985). A popular way of identifying "halos" in such calculations is the friends-of-friends (FOF) algorithm, which links particles within a fraction b of the mean interparticle spacing into one halo, at a density contrast of $\gtrsim 1/b^3$. Other halo identification algorithms generally give similar results. Jenkins et al. (2001) combined the results from simulations with a variety of box sizes to obtain the mass function $n(M)$ of FOF halos over a large dynamic range.

Analytical descriptions of the halo formation process were pioneered by Press & Schechter (1974, hereafter PS) and were recently reviewed by Monaco (1998). Although the PS mass function and its extensions (the so-called excursion set approach, Bond et al. 1991) fit the numerical FOF mass function reasonably well (e.g., Efstathiou et al. 1988), there are real discrepancies both at large and small masses where PS respectively under- and overpredicts halo numbers (e.g., Governato et al. 1999; Jenkins et al. 2001; Bode et al. 2001). Similar discrepancies are found when reproducing the mass function of the progenitors of halos of given mass (Sheth & Lemson 1999; Somerville et al. 2000). In addition, Bond et al. (1991) and White (1996) demonstrated that the PS approach achieves a very poor agreement on an object-by-object basis when compared to simulations (but see Sheth, Mo, & Tormen 2001 for a different view). Analytic approaches based on the peaks of the initial density fields did not achieve a better agreement with simulations (Katz, Quinn, & Gelb 1993). Intermediate between simulations and analytical techniques are perturbative approaches that describe the growth of halos in a *given* numerical realization of a linear density field, such as the truncated Zel'dovich (1970) approximation (Borgani, Coles, & Moscardini 1994), the peak-patch algorithm (Bond & Myers 1996a, 1996b), and the merging cell model (Rodriguez & Thomas 1996; Lanzoni, Mamon, & Guiderdoni 2000).

In this paper we present a new algorithm to compute the formation and evolution of dark matter halos in a given linear density field. A one-dimensional version of this algorithm was given by Monaco & Murante (2000). In common with the other perturbative approaches, we combine a local description of the dynamics in order to identify collapsed halos with Lagrangian perturbation theory to displace the halos to their final positions. We demonstrate that the algorithm leads to an accurate description of the detailed clustering and merger history of halos while requiring several orders of magnitude less computer time and postsimulation analysis than the corresponding full-blown numerical simu-

[1] Dipartimento di Astronomia, Università di Trieste, via Tiepolo 11, 34131 Trieste, Italy.
[2] Institute of Astronomy, Madingley Road, Cambridge CB3 0HA, UK.
[3] SISSA, via Beirut 4, 34014 Trieste, Italy.
[4] Osservatorio Astronomico di Brera, Merate, Italy.
[5] Astronomy Department, University of Washington, Seattle, WA 98195.

lation. In addition, the successful reproduction of the merger history demonstrates that we have identified the key processes that govern halo formation, and that these can be described with a perturbative approach.

We follow a two-step procedure that mimics the hierarchical build-up of halos through accretion and merging. The first step identifies orbit-crossing (OC) as the instant at which a mass element undergoes collapse. We compute OC numerically by applying local ellipsoidal collapse approximation to the full Lagrangian perturbative expansion (Bond & Myers 1996a; Monaco 1995, 1997). This part is the more computationally expensive, requiring several hours of computer time for a 256^3 realization. The second step groups the collapsed particles into disjoint halos, using an algorithm similar to that used to identify halos in N-body simulations. Basically, a particle accretes onto a halo if it is sufficiently close to it at its collapse instant. We use Lagrangian perturbation theory (LPT, Catelan 1995; Bouchet 1996; Buchert 1996) to compute the positions of halos and particles. Seed halos are local maxima of the collapse redshift. This second step automatically determines the full merger history of halos and requires negligible computer time. Compared to simulations, the first step determines when a simulation particle enters a high-density region, whereas the second identifies the halos.

Since our method describes, in the linear density field, the hierarchical build-up of objects that have undergone OC, we refer to it as PINOCCHIO: pinpointing orbit-crossed collapsed hierarchical objects. In the next section we describe the algorithm in more detail. In § 3 we compare its predictions with those from simulations and discuss possible applications of the method. Section 4 gives the conclusions. Technical details and resolution issues are addressed in forthcoming papers (Monaco, Theuns, & Taffoni 2001; Taffoni, Monaco, & Theuns 2001).

2. THE ALGORITHM

2.1. *Orbit Crossing*

Consider a random realization of a density field, $\rho(\boldsymbol{q})$, where $\boldsymbol{q}$ denotes Lagrangian (initial) coordinates, and let $\phi(\boldsymbol{q})$ be the corresponding peculiar potential. Both fields can be smoothed by convolving them with a Gaussian with FWHM R; we denote them as $\rho(\boldsymbol{q}, R)$ and $\phi(\boldsymbol{q}, R)$, respectively. The first derivative of the potential, $\partial_{q_i}\phi$, describes the motion of the particle in the Zel'dovich (1970) approximation, and the shear tensor, $\partial_{q_i}\partial_{q_j}\phi$, can be used to give a description of the deformation of the mass element based on ellipsoidal collapse (Bond & Myers 1996a; Monaco 1995, 1997). In our context, ellipsoidal collapse is a convenient truncation of LPT (Monaco 1997).

For a given smoothing radius R, the density of a mass element will become infinite as soon as at least one of the ellipsoid's axes reaches zero size, at which point the relation $\boldsymbol{x}(\boldsymbol{q})$ becomes multivalued and the Jacobian of the transformation $\boldsymbol{q} \rightarrow \boldsymbol{x}$, $J = \det |\partial \boldsymbol{x}/\partial \boldsymbol{q}| = 0$. This is the definition of OC. We argue that after this instant t_c, nonlinear processes will become important and hence further predictions of what happens to the mass element can not be safely made using LPT. However, as the density of the mass element is already very high, we regard it as a candidate for the building up of a collapsed halo at time $t_c(R)$. A different definition of collapse was used, e.g., by Audit, Teyssier, & Alimi (1997), Lee & Shandarin (1998), and Sheth & Tormen (1999).

In practice we generate the density field ρ on a cubic grid. In our description, mass elements (or "particles") then correspond to the grid vertices $\boldsymbol{q}$. The potential ϕ and its derivatives are computed from ρ using fast Fourier transforms. We typically use ~ 20 logarithmically spaced smoothing radii. Applying local ellipsoidal collapse to each particle, we obtain the collapse redshift on each smoothing scale, and we record for each particle the highest collapse redshift z_c, the corresponding smoothing scale R_c, and the Zel'dovich (1970) estimates for the peculiar velocity $\boldsymbol{v}_c(R_c) \propto \nabla\phi(\boldsymbol{q}, R_c)$ on that smoothing scale. Note that at this stage we make no prediction of the *mass* of the collapsed halo that the particle accreted onto.

In fact, the collapsed mass element will not necessarily have accreted onto any halo, but may instead have become part of a filament or sheet (collectively referred to as "filaments" hereafter), since these have undergone OC as well. These structures trace the moderate over-densities that connect the much higher density collapsed halos in simulations. The next subsection describes how the OC region is divided into collapsed halos and OC filaments.

2.2. *Fragmentation*

The grouping of OC particles into halos mimics the hierarchical formation of objects, and also the way in which halo finders identify collapsed objects in simulations. We begin by sorting particles according to decreasing collapse redshift, z_c, and starting from the highest z_c we decide the fate of the collapsed particle, working our way down, forward in time to the last particle to collapse.

Briefly, at the instant the particle is deemed to collapse, we decide which halo, if any, it accreted onto. The candidate halos are those that already contain one Lagrangian neighbor of the particle.[6] The particle will accrete onto the halo if it is sufficiently close to it at the collapse time, mimicking the construction of FOF halos. We use the Zel'dovich velocities $\boldsymbol{v}_c$ as defined earlier to compute the distance, at the collapse time, between the particle and the candidate halo. If a particle has more than one candidate halo, we also check whether these halos should merge, using a similar merger criterion. Notice that in this way halos are by construction connected regions in Lagrangian space.

More in detail, we apply the following rules for accretion and merging. (Lengths are in units of the grid spacing; $R_M = M^{1/3}$ is the "radius" of a halo of M particles.)

1. *Seed halos*—Local maxima of the collapse redshift z_c are seeds for a new halo.

2. *Accretion*—A collapsing particle (not a local maximum) accretes onto a candidate halo (i.e., containing one of its Lagrangian neighbors) if the distance d, at the collapse time between particle and halo center-of-mass is $d \leq f_a R_M$. The quantity f_a is a parameter of order unity, analogous to the linking-length parameter used to identify FOF halos. If the particle is able to accrete onto two (or more) halos, we assign it to the one for which d/R_M is the smallest.

3. *Merging*—If the particle has more than one candidate halo, then these halos are merged if their mutual distance d, again at the particle's collapse time, is $d \leq f_m R_M$, where R_M refers to the larger halo and f_m is again a parameter of order

[6] On the initial grid $\boldsymbol{q}$ of Lagrangian positions, the six particles nearest to a given particle are its Lagrangian neighbors.

unity. Since we only consider six Lagrangian neighbors, up to six halos may merge at a given time, although binary and ternary mergers are of course much more frequent.

4. *Filaments*—With these rules for accretion and merging, some collapsing particles do not accrete onto a halo at their collapse time. Since these particles tend to occur in the mildly over-dense regions that connect the halos (visible as a filamentary network between halos in simulations), we assign them to a "filaments" group. In N-body simulations, some particles accrete onto a halo directly from this filamentary network, *without* passing through a collapsed halo first. In order to account for this, we check the Lagrangian neighbors of a particle that accretes onto a halo according to the accretion condition (2). If any of these neighbors already belong to the filaments group, then they also accrete onto that halo. (So up to five additional particles may accrete onto the halo, if their common Lagrangian neighbor satisfies condition [2]).

When the groups are very small, R_M is comparable to the grid spacing, and the Zel'dovich displacements are often not sufficiently accurate for the accretion or merging condition to be fulfilled. This resolution effect results in producing too few small halos at high redshift. To remedy this we improve the accretion condition to $d < f_a R_M + f_r$, and similarly for merging. Our algorithm thus contains three parameters (f_a, f_m, and f_r) which need to be calibrated using the FOF mass function as determined from a simulation, and which have obvious physical interpretations in terms of accretion, merging and resolution effects. Optimal values are $f_a = 0.18$, $f_m = 0.35$, and $f_r = 0.7$. These values were obtained by comparing the PINOCCHIO mass function with those of several simulations, including the standard SCDM one discussed below, a ΛCDM simulation ($\Omega_m = 0.3$, $\Omega_\Lambda = 0.7$, $\sigma_8 = 1$, $h = 0.7$) run with the same simulation code and box size (500 h^{-1} Mpc) and another ΛCDM simulation ($\Omega_\Lambda = 0.7$, $\Omega_m = 0.3$, $\sigma_8 = 0.9$, $h = 0.65$) with different resolutions (128^3 and 256^3 particles) in a smaller box of 100 h^{-1} Mpc, evolved with the P3M HYDRA code (Couchman 1991). The agreement between PINOCCHIO and these other simulations is as good as the comparison with the SCDM simulation described in the next section; the best fit parameters are found to agree within ~ 0.01. However, at smaller and more nonlinear scales, more subtle resolution effects appear for which corrections can be made. These details will be discussed in the forthcoming paper Monaco et al. (2001).

3. RESULTS

We have applied PINOCCHIO to the initial conditions of a simulation by Governato et al (1999). This large-volume, dissipationless simulation uses 360^3 dark matter particles and was evolved using the PKDGRAV tree code (comoving box size 500 h^{-1} Mpc, matter density $\Omega_m = 1$, Hubble constant $H_0 = 50$ km s^{-1} Mpc^{-1}, standard CDM spectrum with $\sigma_8 = 1$). Halos have been identified at several output times using a standard FOF algorithm with linking length $b = 0.2$. PINOCCHIO is fast: Resampling the initial conditions onto a 256^3 grid, the first stage of computing orbit-crossing requires $\sim$ 6 hours of CPU time; the second step of identifying the halos takes just a few minutes. (Timings refer to a Pentium III 450 MHz personal computer. Memory requirement in this case amounts to ~ 512 megabytes of RAM). These timings should be contrasted with the several hundreds of hours on 256 nodes of a T3E Cray supercomputer required to perform the original simulation. Moreover, PINOCCHIO immediately outputs the merger tree of each halo, which should be contrasted to the complicated and expensive postprocessing necessary to extract merger trees from a simulation.

One way to understand the large speed-up between an N-body simulation and PINOCCHIO is that most of the CPU time used in the N-body simulation is spent integrating the orbits for particles *already inside a halo*. These particles undergo large accelerations as they orbit inside the halo, and hence may require thousands of time steps in order for their orbits to be integrated accurately. PINOCCHIO, on the other hand, completely ignores particles once they are inside a halo and so can use far fewer steps per particle to perform the whole simulation, since it only needs to compute the particle's orbit *before* it enters any high-density region. Obviously, all information on the internal structure of the halo is lost in the process, but it is well known that several millions of particles are required to get the internal structure correct. (See the controversy about the slope of halo profiles as determined using high-resolution collisionless simulations, e.g., Ghingha et al. 2000.) In the following, we demonstrate that PINOCCHIO is indeed able to predict the merging and clustering properties of halos very accurately.

PINOCCHIO reproduces the mass function $Mn(M)$ (number of objects per unit volume and unit $\ln M$) to better than 10% at all redshifts (Fig. 1) in the mass range in which halos have at least ~ 30 particles and Poisson error bars are small. To make this more evident, we plot in the lower panel of Figure 1 the residuals with respect to the $z = 0$ FOF mass function. This level of accuracy improves over the fit proposed by Sheth & Tormen (1999). The PS mass function, which over- (under-) predicts the number of low- (high-) mass objects, is shown for comparison as well.

The good agreement between halo masses is not just statistical in nature. We have plotted in Figure 2 the masses of the halos that a particle is assigned to, for both PINOCCHIO and FOF halos, for a random subset of particles drawn from the initial conditions. The correlation between PINOCCHIO and FOF masses is extremely tight and is dramatically better than PS (compare with Fig. 2 in Sheth et al. 2001), and also improves over peak-patch (Bond & Myers 1996b, their Fig. 11).

Figure 2 contains outliers which correspond to particles that are assigned to a different halo (or are not assigned to a halo at all) by PINOCCHIO than by the simulation (or vice versa). We have investigated in detail the typical overlap in the initial conditions between simulated halos and those found by PINOCCHIO. Since PINOCCHIO refers to the same initial conditions as the simulation, we can determine the fraction of Lagrangian volume $V_{\rm P}$ of a given halo identified by PINOCCHIO that overlaps the Lagrangian volume $V_{\rm FOF}$ of a FOF halo. In general, for any FOF halo, the volume $V_{\rm FOF}$ may overlap with the Lagrangian volumes of several PINOCCHIO halos (and vice versa). For example, if two PINOCCHIO halos fail to merge, whereas the corresponding FOF halos do merge, then the volume $V_{\rm FOF}$ may be broken up into two PINOCCHIO volumes $V_{\rm P}$. We choose to pair up two halos between the two catalogs if their Lagrangian volumes overlap to better than 30%. Paired-up halos are in addition called "cleanly assigned" if the intersection of $V_{\rm FOF}$ with $V_{\rm P}$ is larger than for any other FOF halo, and vice versa. Paired-up halos that are not

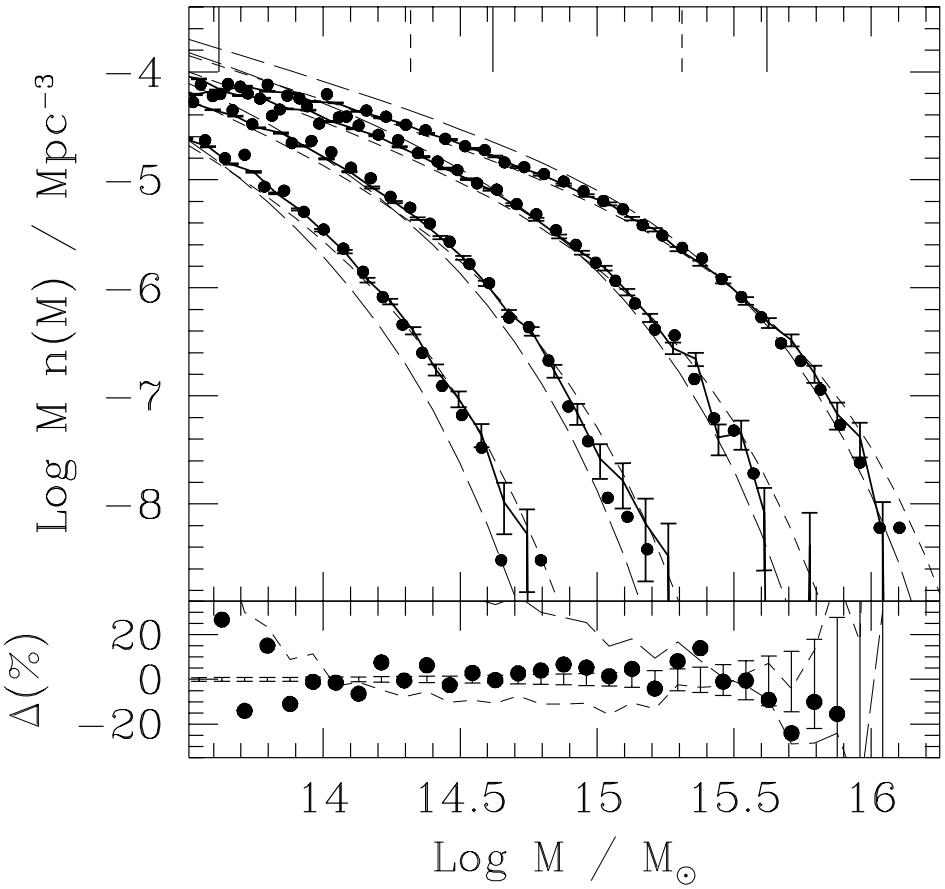

FIG. 1.—Comparison of mass function $Mn(M)$ in a standard CDM model ($\Omega_m = 1$). *Top panel*: Simulated mass function for FOF selected halos (*solid lines with Poissonian error bars*), PINOCCHIO mass function (*filled circles*), the fit by Sheth & Tormen (*short dashed lines*), and PS function (*long dashed lines*), at redshifts $z = 0$, 0.43, 1.13, and 1.86 (higher redshift curves are offset by 0.1 dex both vertically and horizontally for improved clarity). Vertical lines show limits corresponding to simulation halos with 10, 50, 100, 500, and 1000 particles (256^3 resampling). *Bottom panel*: Difference between simulated mass function and PINOCCHIO (*filled dots*), Sheth & Tormen fit (*short dashed line*), and PS (*long dashed line*) at $z = 0$.

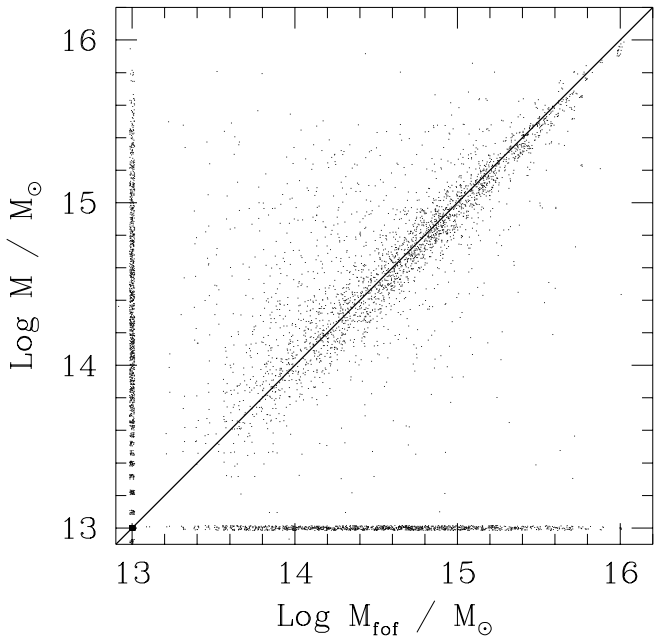

FIG. 2.—Predicted halo mass against FOF halo mass for a subset of the particles of Governato et al. (1999) $\Omega_m = 1$ simulation at redshift $z = 0$. The PINOCCHIO masses are highly correlated with the FOF masses. Points which have not collapsed have been arbitrarily assigned a mass of $10^{13} M_\odot$.

cleanly assigned are called "split." Denoting the fraction of halos that are cleanly assigned and the fraction that are split by $f_{\rm cl}$ and $f_{\rm split}$, respectively, then the fraction of halos that are not paired up is obviously $1 - f_{\rm cl} - f_{\rm split}$.

In Figure 3, we show $f_{\rm cl}$ and $f_{\rm split}$ as a function of halo mass for several redshifts. For sufficiently massive halos $M \geq 10^{14} M_\odot$ (corresponding to 40 particles), $f_{\rm cl} \geq 0.8$, showing that most FOF halos can be unambiguously associated with a corresponding PINOCCHIO halo, while the fraction of FOF halos split in two or more PINOCCHIO halos is small. The fraction $1 - f_{\rm cl} - f_{\rm split}$ of FOF halos that have no corresponding PINOCCHIO halo is very small as well, ranging from $\lesssim 1\%$ for the most massive halos, to $\sim 15\%$ for small halos with ~ 40 particles. The latter limit is close to the minimum number needed to correctly numerically simulate the formation of a halo, given an initial density field. For cleanly assigned halos, the bottom panel in the figure shows the fractional overlap $f_{\rm ov}$ of the respective Lagrangian volumes. A typical value for well-resolved halos is $f_{\rm ov} \sim 0.7$, indicating that the mass errors are usually smaller than 30%. This is made more clear in Figure 4, which compares the FOF with the PINOCCHIO masses for cleanly assigned halo pairs. The correlation is very tight. The level of agreement between PINOCCHIO and simulations is only weakly dependent on redshift.

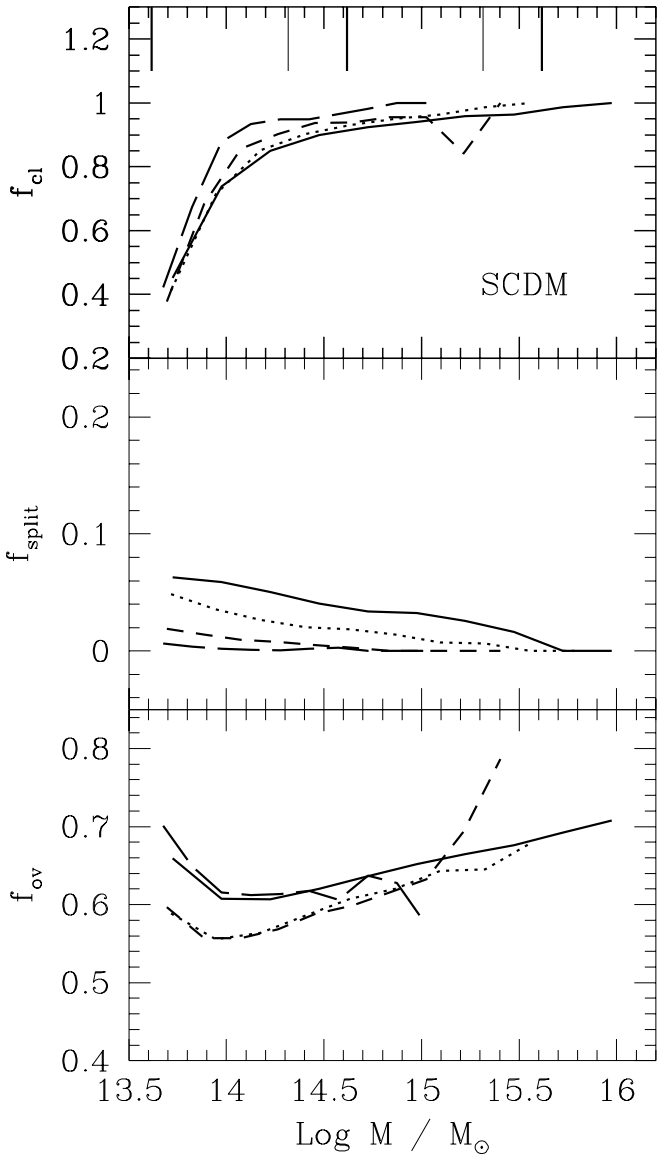

FIG. 3.—Statistics of halo overlap between PINOCCHIO and FOF objects for halos at $z = 0$ (*solid lines*), $z = 0.43$ (*dotted lines*), $z = 1.13$ (*short dashed lines*), and $z = 1.86$ (*long dashed lines*). *Upper panel*: Fraction f_{cl} of "cleanly assigned" halo pairs between the two catalogs, as a function of mass. *Middle panel*: fraction f_{split} of FOF halos that are split in two PINOCCHIO halos. *Lower panel*: Average overlap in Lagrangian space, f_{ov}, for cleanly paired-up halos. (See text for definitions of f_{cl} and f_{split}.) As in Figure 1, vertical lines show limits corresponding to simulation halos with 10, 50, 100, 500, and 1000 particles (256^3 resampling).

Since PINOCCHIO halos are very similar in detail to their corresponding FOF halos, their merging history and clustering properties can be expected to be very similar as well. The conditional mass function $n(M, z \mid M_0, z_0)$ (the number density of objects of mass M at redshift z that are merged in halos of mass M_0 at the later redshift z_0) is shown in Figure 5. The PS prediction, computed following Bond et al. (1991; see also Bower 1991; Lacey & Cole 1993) is also shown. Also in this case the agreement between PINOCCHIO and the simulation is very good, making an improvement with respect to PS and demonstrating that PINOCCHIO halos undergo a very similar merging history as do FOF halos.

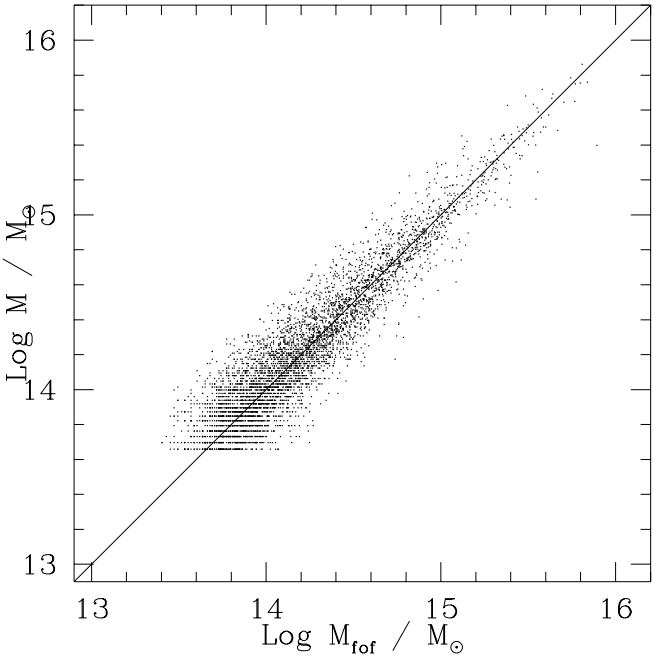

FIG. 4.—PINOCCHIO vs. FOF halo masses for objects that were cleanly assigned between the two respective catalogs. Note that each dot corresponds to a halo pair, which contrasts with Figure 2, where each dot refers to a *random* point in the initial conditions.

Finally, we compare in Figure 6 the two-point correlation function $\xi(r)$ of halos as a function of mass and redshift. The agreement with the simulations is again very good. In particular, the high clustering amplitude of massive halos at early times is well-reproduced, and the correlation length r_0 is recovered to within 10% or better, thus improving the PS-like estimate of Sheth et al. (2001) and allowing easy discrimination between different cosmological models (Colberg et al. 2000). The quality of this

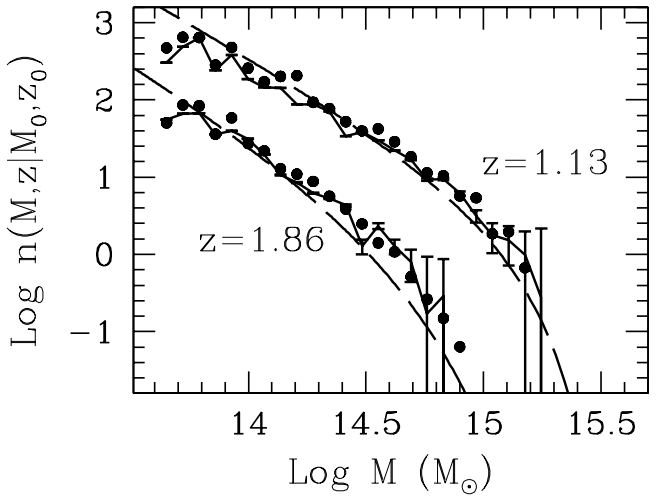

FIG. 5.—Conditional mass function of halos with mass $M_0 = 5 \times 10^{15}\ M_\odot$ at redshift $z = 0$, at the earlier redshifts 1.13 and 1.86 as indicated. Solid lines with Poissonian error bars are for the simulation, filled circles correspond to the PINOCCHIO prediction, long dashed lines are the conditional mass function from the PS theory (Bower 1991). The higher redshift results have been offset vertically by 1 dex for clarity. The PINOCCHIO mass function follows the simulations significantly better than the PS one.

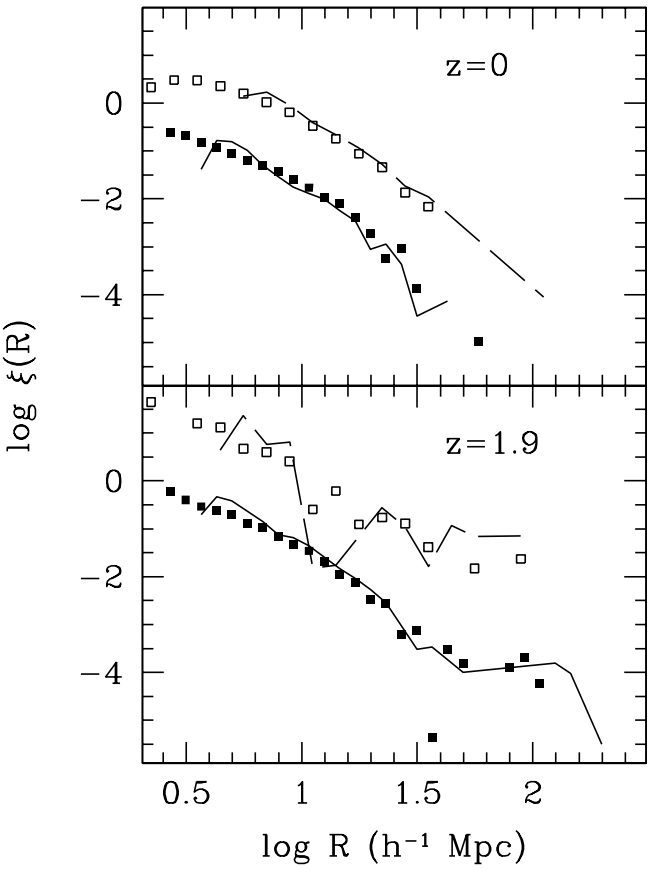

FIG. 6.—Correlation functions for halos within a given mass range as a function of comoving separation R for the two redshifts indicated in the panels. Symbols refer to FOF selected halos, lines to PINOCCHIO halos. Mass ranges are $10^{14} \leq \log M/M_{\odot} \leq 10^{14.5}$ (*filled squares and full lines*) and $\log M/M_{\odot} \geq 10^{14.5}$ (*open squares and dashed lines respectively*). Lower mass curves have been offset vertically by 1 dex for clarity. The number of contributing halos for the lower mass range is $\approx 41 \times 10^3$ and 12×10^3 (for increasing redshifts), for the higher mass range 19×10^3 and 0.5×10^3.

agreement suggests that halo positions are well-estimated by PINOCCHIO; we find that the one−dimensional rms error on the final positions is $\sim 0.8\ h^{-1}$ Mpc (smaller than the grid spacing), while velocities are recovered with a one-dimensional rms of ~ 150 km s^{-1}.

4. CONCLUSIONS

We have demonstrated that PINOCCHIO is able to accurately describe the evolution of clustering of halos as a function of mass. Therefore, when combined with semi-analytical models for galaxy formation (White & Frenk 1991; Kauffmann, White, & Guiderdoni 1993; Cole et al 1994; Somerville & Primack 1999), PINOCCHIO can be used to reliably generate mock galaxy catalogs, with the correct evolution of galaxy clustering built in, while requiring orders of magnitude less computer time than numerical simulations. Easy and accurate production of large halo catalogues is invaluable for interpreting data and estimating errors from galaxy or galaxy cluster surveys; for example, when studying galaxy bias (Diaferio et al. 1999; Benson et al. 2000), estimating power spectra (e.g., Efstathiou & Moody 2001), determining shear from weak lensing measurements (van Waerbeke et al. 1999; Wittman et al. 2000; Bacon, Refregier, & Ellis 200; Kaiser, Wilson, & Luppino 2000), or studying intrinsic galaxy alignments (Crittenden et al. 2001; Brown et al. 2000).

A more detailed and technical account of the code, suitable for those who wish to use it, will be given in a forthcoming paper (Monaco et al. 2001), while the ability of predicting halo merger histories beyond the progenitor mass function will be presented by Taffoni et al. (2001). A public version of PINOCCHIO is available.[7]

We thank Jasjeet Bagla, Stefano Borgani, Anatoly Klipin, Barbara Lanzoni, Sergei Shandarin, and Ravi Sheth for many discussions. N-body simulations were run at the ARSC and Pittsburg supercomputing centers. P. M. acknowledges support from MURST. T. T. acknowledges support from the "Formation and Evolution of Galaxies" network set up by the European Commission under contract ERB FMRX-CT96086 of its TMR program, and from PPARC for the award of postdoctoral fellowship. Research conducted in cooperation with Silicon Graphics/Cray Research utilizing the Origin 2000 supercomputer at DAMTP, Cambridge.

[7] A public version of PINOCCHIO is available at the site http://www.daut.univ.trieste.it/pinocchio.

REFERENCES

Audit, E., Teyssier, R., & Alimi, J. M. 1997, A&A, 325, 439
Benson, A. J., Cole, S., Frenk, C. S., Baugh, C. M., & Lacey, C. G. 2000, MNRAS, 311, 793
Bode, P., Bahcall, N. A., Ford, E. B., & Ostriker, J. P. 2001, ApJ, 551, 15
Bond, J. R., Cole, S., Efstathiou, G., & Kaiser, N. 1991, ApJ, 379, 440
Bond, J. R., & Myers, S. T. 1996a, ApJS, 103, 1
———. 1996b, ApJS, 103, 41
Borgani, S., Coles, P., & Moscardini, L. 1994, MNRAS, 271, 223
Bouchet, F. 1996, in Dark Matter in the Universe, ed. S. Bonometto et al. (Amsterdam: IOS), 565
Brown, M. L., Taylor, A. N., Hambly, N. C., & Dye, S. 2000, MNRAS, submitted (astro-ph/0009499)
Buchert, T. 1996, in Dark Matter in the Universe, ed. S. Bonometto et al. (Amsterdam: IOS), 543
Catelan, P. 1995, MNRAS, 276, 115
Colberg, J. M., et al. 2000, MNRAS, 319, 209
Cole, S., Aragon-Salamanca, A., Frenk, C. S., Navarro, J. F., & Zepf, S. E. 1994, MNRAS, 271, 781
Couchman, H.M.P. 1991, ApJ, 368, L23
Crittenden, R. G., Natarajan, P., Pen, U., & Theuns, T. 2001, ApJ, 559, 552
Diaferio, A., Kauffmann, G., Colberg, J. M., & White, S. D. M. 1999, MNRAS, 307, 537
Efstathiou, G., Davis, M., White, S. D. M., & Frenk, C. S. 1985, ApJS, 57, 241
Efstathiou, G., Frenk, C. S., White, S. D. M., & Davis, M. 1988, MNRAS, 235, 715
Efstathiou, G., & Moody, S. 2001, MNRAS, 325, 1603
Ghigna, S., Moore, B., Governato, F., Lake, G., Quinn, T., & Stadel, J. 2000, ApJ, 544, 616
Governato, F., Babul, A., Quinn, T., Tozzi, P., Baugh, C. M., Katz, N., & Lake, G. 1999, MNRAS, 307, 949
Jenkins, A., Frenk, C. S., White, S. D. M., Colberg, J.M., Cole, S., Evrard, A. E., Couchman, H. M. P., & Yoshida, N. 2001, MNRAS 321, 372
Kaiser, N., Wilson, G., & Luppino, G.A. 2000, ApJL, submitted (astro-ph/0003338)
Katz, N., Quinn, T., & Gelb, J. M. 1993, MNRAS, 265, 689
Kauffmann, G., White, S. D. M., & Guiderdoni, B. 1993, MNRAS, 264, 201
Lacey, C., & Cole, S. 1993, MNRAS, 262, 627
Lanzoni, B., Mamon, G. A., & Guiderdoni, B. 2000, MNRAS, 312, 781
Lee, J., & Shandarin, S.F. 1998, ApJ, 500, 14
Monaco, P. 1995, ApJ, 447, 23
———. 1997, MNRAS, 287, 753
———. 1998, Fundam. Cosm. Phys., 19, 153
Monaco, P., & Murante, G. 2000, Phys. Rev. D, 60, 0635XX

Monaco, P., Theuns, T., & Taffoni, G. 2001, MNRAS, submitted (astro-ph/0109323)
Peebles, P. J. E. 1993, in Principles of Physical Cosmology (Princeton: Princeton Univ. Press)
Press, W. H., & Schechter, P. 1974, ApJ, 187, 425 (PS)
Rees, M. J., & Ostriker, J. P. 1977, MNRAS, 179, 541
Rodrigues, D. D. C., & Thomas, P. A. 1996, MNRAS, 282, 631
Sheth, R. K., & Lemson, G. 1999, MNRAS, 305, 946
Sheth, R. K., Mo, H., & Tormen, G. 2001, MNRAS, 323, 1
Sheth, R. K., & Tormen, G. 1999, MNRAS, 308, 119
Somerville, R. S., Lemson, G., Kolatt, T. S., & Dekel A. 2000, MNRAS, 316, 479
Somerville, R. S., & Primack J. R. 1999, MNRAS, 310, 1087
Taffoni, G., Monaco, P., & Theuns, T. 2001, MNRAS, submitted (astro-ph/0109324)
van Waerbeke, L., Bernardeau, F., & Mellier, Y. 1999, A&A, 342, 15
White, S. D. M. 1996, in Les Houches, Session LX, Cosmology & Large-Scale Structure, ed. R. Schaeffer et al. (Amsterdam: Elsevier), 349
White, S. D. M., & Frenk, C. S. 1991, ApJ, 379, 52
White, S. D. M., & Rees, M. J. 1978, MNRAS, 183, 341
Wittman, D. M., Tyson, J. A., Kirkman, D., Dell'Antonio, I., & Bernstein, G. 2000, Nature, 405, 1
Zel'dovich Y. A. B. 1970, Astrofizika, 6, 319 (translated in Astrophysics, 6, 164 [1973])